

DFT Study on Alkyl- and Haloborylene Complexes of Manganese and Rhenium: Structure and Bonding Energy Analysis in $[(\eta^5\text{-C}_5\text{H}_5)(\text{CO})_2\text{M}(\text{BR})]$ and $[(\eta^5\text{-C}_5\text{H}_5)(\text{CO})_2\text{M}(\text{BX})]$ ($\text{M} = \text{Mn, Re}$; $\text{R} = \text{Me, Et, } i\text{Pr, } t\text{Bu}$; $\text{X} = \text{F, Cl, Br, I}$)

Krishna K. Pandey,^{*[a]} Holger Braunschweig,^{*[b]} and Rian D. Dewhurst^[b]

Keywords: Manganese / Rhenium / Boron / Boron ligand / Borylene complex / Density functional calculations

Electronic, molecular structures, and bonding analysis of the terminal neutral alkylborylene and haloborylene complexes of manganese and rhenium $[(\eta^5\text{-C}_5\text{H}_5)(\text{CO})_2\text{M}(\text{BR})]$ and $[(\eta^5\text{-C}_5\text{H}_5)(\text{CO})_2\text{M}(\text{BX})]$ ($\text{M} = \text{Mn, Re}$; $\text{R} = \text{Me, Et, } i\text{Pr, } t\text{Bu}$; $\text{X} = \text{F, Cl, Br, I}$) were investigated at the DFT/BP86/TZ2P level of theory. The calculated geometry of the manganese alkylborylene complex $[(\eta^5\text{-C}_5\text{H}_5)(\text{CO})_2\text{Mn}(t\text{Bu})]$ is in excellent agreement with the experimentally derived structural data. Pauling bond order of the optimized structures shows that the M–B bonds in these complexes are almost M=B double bonds, which is also supported by the performed energy decomposition analysis. The orbital interactions between the metal and boron arise mainly from $\text{M} \leftarrow \text{BR}$ σ donation, while the π bonding contribution is relatively small (22.6–25.8 % of total orbital contributions). The M–B π bond orbitals are highly polarized towards the metal atom and the contributions of boron are very small. In the BX ligands, σ bonding, interaction energies, electrostatic interactions and bond

dissociation energies are smaller than those in the BR ligands. The contributions of the electrostatic interactions ΔE_{elstat} are significantly larger in all borylene complexes than the covalent bonding ΔE_{orb} : the $[\text{M}]=\text{BR}$ bonding in the alkylborylene and haloborylene complexes has a greater degree of ionic character (ca. 61.7 % for the complexes **I–IV**, ca. 65.7 % for the complexes **V–VIII**, 53.9–56.2 % for the complexes **IX–XII** and 58.5–60.4 % for the complexes **XIII–XVI**). The chloroborylene complexes $[(\eta^5\text{-C}_5\text{H}_5)(\text{CO})_2\text{M}(\text{BCl})]$ possess the highest electrostatic interactions, ΔE_{elstat} of all haloborylene complexes $[(\eta^5\text{-C}_5\text{H}_5)(\text{CO})_2\text{M}(\text{BX})]$, whereas the iodoborylene complexes $[(\eta^5\text{-C}_5\text{H}_5)(\text{CO})_2\text{M}(\text{BI})]$ display the highest orbital interactions, ΔE_{orb} . The dimerization of the terminal borylene complex $[(\eta^5\text{-C}_5\text{H}_5)(\text{CO})_2\text{Mn}(\text{BCl})]$ to $[(\eta^5\text{-C}_5\text{H}_5)(\text{CO})_2\text{Mn}]_2(\eta\text{-}\eta\text{-}\mu\text{-B}_2\text{Cl}_2)$ is a strongly exothermic process (21.04 kcal/mol below the starting monomers) and the energies are in favor of a dimerization reaction.

Introduction

The history of organometallic chemistry owes much to the fragment $[(\eta^5\text{-C}_5\text{R}_5)\text{M}(\text{CO})_2]$ ($\text{M} = \text{Mn, Re}$). This neutral, 16VE organometallic scaffold has a distinguished record of stabilizing some of the earliest examples of organometallic species. Fischer and co-workers^[1a] synthesized some early examples of alkylidene complexes featuring this fragment, and later the first examples of cationic alkylidyne complexes.^[1b] Similarly, a number of complexes featuring bridging, low-valent organometallic and main group ligands were synthesized featuring two $(\eta^5\text{-C}_5\text{R}_5)\text{Mn}(\text{CO})_2$ fragments, such as the first parent alkylidene complex (“ $\mu\text{-CH}_2$ ”, Herrmann et al.),^[2a] a stannylidene complex (“ $\mu\text{-$

SnR_2 ”, Ulrich et al.),^[2b] and an anionic “germanium-inidene” complex (“ $\mu\text{-GeI}$ ”, Huttner et al.).^[2c]

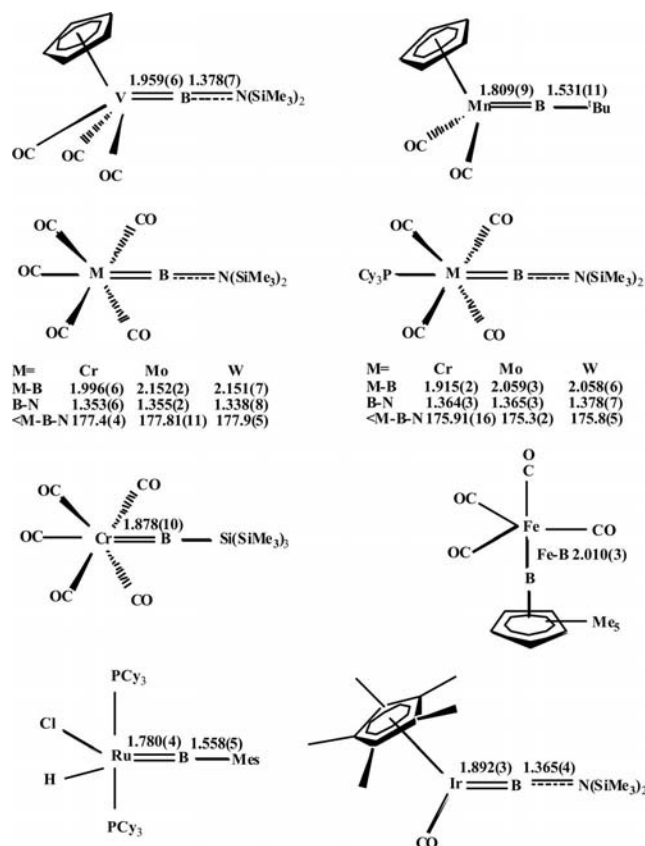
Similarly, the field of boron-transition metal chemistry has benefitted from the remarkable stability that the $[(\eta^5\text{-C}_5\text{R}_5)\text{M}(\text{CO})_2]$ fragment can bestow upon a complex. The first bridging borylene complexes,^[3] as well as the only known terminal alkyl borylene complex,^[4] all partly owe their stability to the properties of the manganese fragment. In terms of transition metal borylene chemistry, twelve structurally characterized neutral terminal transition metal borylene complexes (Scheme 1)^[4–14] and nine terminal cationic transition metal borylene complexes (Scheme 2)^[15–22] have been reported. Additionally, a number of base-stabilized adducts formed by the coordination of a Lewis base (main group or transition metal) to the two- or three-coordinate boron center have also been prepared. These families of neutral, cationic and base-stabilized borylene complexes have been summarized in recent reviews on the topic.^[23–33]

It is apparent from Schemes 1 and 2 (and as has been reported^[33]) that terminal borylene complexes require either steric protection or π -electron donation from the borylene substituent in order to be stable enough to be isolated. For

[a] School of Chemical Sciences, Devi Ahilya University Indore, Indore 452017, India
E-mail: kkpandey.schem@dauniv.ac.in

[b] Institut für Anorganische Chemie, Julius-Maximilians-Universität Würzburg, Am Hubland, 97074 Würzburg, Germany
Fax: +49-931-8884623
E-mail: h.braunschweig@mail.uni-wuerzburg.de

Supporting information for this article is available on the WWW under <http://dx.doi.org/10.1002/ejic.201001200>.

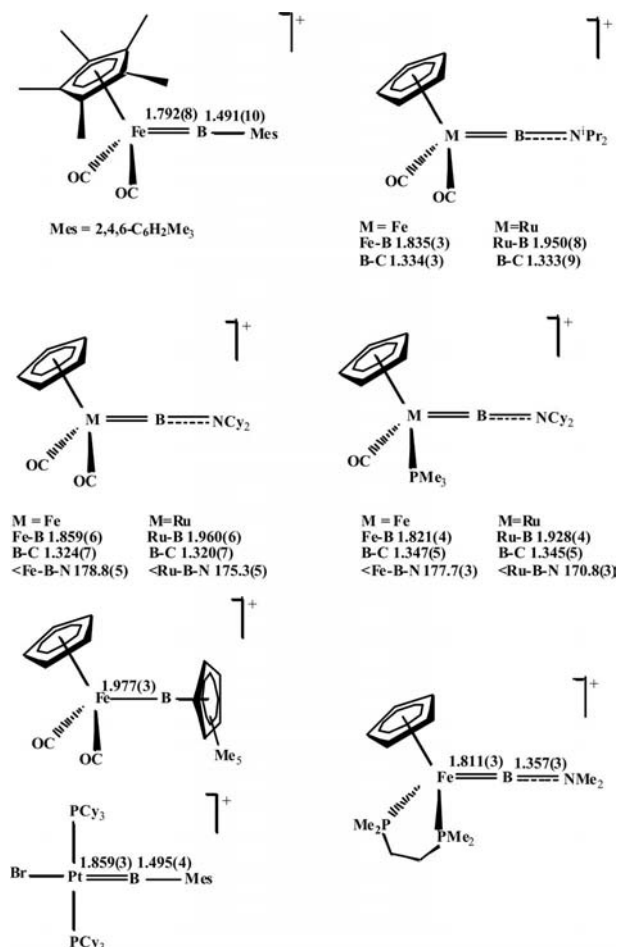


Scheme 1. Selected structurally characterized neutral terminal metal borylene complexes.

instance, no terminal alkylborylene complexes are known with substituents smaller than *tert*-butyl, and terminal haloborylene complexes are yet to be isolated. Accordingly, we have attempted a computational study of these two classes of complex in order to gain insight into the properties of these hypothetical species, and report the geometry, electronic structure and nature of the M–B bonds in these complexes.

One promising synthetic route to a terminal haloborylene complex was the reaction of $[(\eta^5\text{-C}_5\text{H}_5)(\text{CO})_2\text{Mn}_2(\mu\text{-BCl})]$ with CO, however this reaction resulted in the formation of the dinuclear manganese complex $[(\eta^5\text{-C}_5\text{H}_5)(\text{CO})_2\text{Mn}_2(\eta^2\text{-}\mu\text{-B}_2\text{Cl}_2)]$, presumably by dimerization of the intermediate terminal chloroborylene complex.^[34] Accordingly, we have computationally determined the mechanism for the formation of the dinuclear manganese complex $[(\eta^5\text{-C}_5\text{H}_5)(\text{CO})_2\text{Mn}_2(\eta^2\text{-}\mu\text{-B}_2\text{Cl}_2)]$. Given the relative stability of the terminal alkylborylene $[(\eta^5\text{-C}_5\text{H}_5)\text{M}(\text{CO})_2(\text{B}t\text{Bu})]$, and the aforementioned history of such fragments, we chose $[(\eta^5\text{-C}_5\text{H}_5)\text{M}(\text{CO})_2]$ (M = Mn, Re) as a scaffold for our computational models of complexes with alkyl- (B–R; R = Me, Et, *i*Pr, *t*Bu) and haloborylene (B–X; X = F, Cl, Br, I) ligands.

Theoretical approaches have become an indispensable part of the studies of terminal metal borylene complexes.^[35–44] Previously, the BLYP/LANL2DZ and B3LYP/LANL2DZ approaches have been applied to study the



Scheme 2. Selected structurally characterized cationic terminal metal borylene complexes.

geometry and electronic structure of terminal cationic borylene complexes $[(\eta^5\text{-C}_5\text{H}_5)(\text{CO})_2\text{Fe}\{\text{B}(\eta^5\text{-C}_5\text{Me}_5)\}]^+$, $[(\eta^5\text{-C}_5\text{H}_5)(\text{CO})_2\text{Fe}(\text{BMe}_3)]^+$, $[(\eta^5\text{-C}_5\text{H}_5)(\text{CO})_2\text{Fe}(\text{BNMe}_2)]^+$ and $[(\eta^5\text{-C}_5\text{H}_5)(\text{CO})_2\text{Ru}(\text{BNMe}_2)]^+$.^[16,20,21,45] Structure and bonding energy analysis of borylene complexes of iron, ruthenium and osmium^[46] and of cobalt, rhodium and iridium^[47] have been studied in detail. For our model systems, we have investigated the degree of ionic and covalent character of the M=B bonds as well as the M←B σ bonding and the M→B π back bonding contributions to the M=B bonds (see Figure 1 for schematic presentation of M=BR and M=BX bonds).

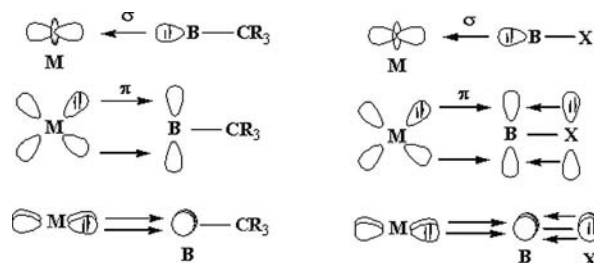


Figure 1. Schematic representation of the M–BCR₃ and M–BX orbital interactions.

Computational Details

Calculations of the neutral terminal alkyl- and haloborylene complexes $[(\eta^5\text{-C}_5\text{H}_5)(\text{CO})_2\text{Mn}(\text{BR})]$ (I, R = Me; II, R = Et; III, R = *i*Pr; IV, R = *t*Bu), $[(\eta^5\text{-C}_5\text{H}_5)(\text{CO})_2\text{Re}(\text{BR})]$ (V, R = Me; VI, R = Et; VII, R = *i*Pr; VIII, R = *t*Bu), $[(\eta^5\text{-C}_5\text{H}_5)(\text{CO})_2\text{Mn}(\text{BX})]$ (IX, X = F; X, X = Cl; XI, X = Br; XII, X = I), $[(\eta^5\text{-C}_5\text{H}_5)(\text{CO})_2\text{Re}(\text{BX})]$ (XIII, X = F; XIV, X = Cl; XV, X = Br; XVI, X = I) as well as bridged borylene complexes $[\{(\eta^5\text{-C}_5\text{H}_5)(\text{CO})_2\text{Mn}\}_2(\mu\text{-BCl})]$ (XVII), $[\{(\eta^5\text{-C}_5\text{H}_5)(\text{CO})_2\text{Mn}\}_2(\mu\text{-BCl})(\mu\text{-CO})]$ (XVIII), $[\{(\eta^5\text{-C}_5\text{H}_5)(\text{CO})_2\text{Mn}\}_2(\mu\text{-BCl})_2]$ (transition state) (XIX) and $[\{(\eta^5\text{-C}_5\text{H}_5)(\text{CO})_2\text{Mn}\}_2(\eta^1\eta^1\mu\text{-B}_2\text{Cl}_2)]$ (XX) have been performed at the nonlocal DFT level of theory using the exchange functional of Becke^[48] and the correlation functional of Perdew^[49] (BP86). Scalar relativistic effects have been considered using the ZORA formalism.^[50] Uncontracted Slater-type orbitals (STOs) using triple- ζ basis sets augmented by two sets of polarization functions were employed for the SCF calculations.^[51] The $(1s)^2$ core electrons of boron, carbon, oxygen and fluorine, $(1s2s2p)^{10}$ core electrons of chlorine and manganese, $(1s2s2p3s3p)^{18}$ core electrons of bromine, $(1s2s2p3s3p3d4s4p)^{36}$ core electrons of iodine and $(1s2s2p3s3p3d4s4p4d)^{46}$ core electrons of rhenium were treated by the frozen-core approximation.^[52] An auxiliary set of s, p, d, f and g STOs was used to fit the molecular densities and to present the coulomb and exchange potentials accurately in each SCF cycle.^[53] The calculations were performed utilizing the program package ADF-2008.01.^[54]

The binding between the metal $[(\eta^5\text{-C}_5\text{H}_5)(\text{CO})_2\text{M}]$ (singlet state) and alkylborylene BR/haloborylene BX (singlet state) fragments in complexes I–XVI has been analyzed at the C_s symmetry using the energy decomposition scheme of ADF package which is based on the Morokuma^[55] and Ziegler and Rauk^[56] methods. Based on these studies, the bond energy ΔE between the fragments can be decomposed as shown in Equation (1).

$$\Delta E = \Delta E_{\text{int}} + \Delta E_{\text{prep}} \quad (1)$$

ΔE_{prep} is the energy required to promote the free fragments from their equilibrium structure of the electronic ground

state into that which they take up in the molecule, see Equation (2).

$$\Delta E_{\text{prep}} = E_{\text{total}}(\text{distorted fragments}) - E_{\text{total}}(\text{fragments in the equilibrium structure}) \quad (2)$$

In Equation (1), ΔE_{int} is the instantaneous interaction energy between the two fragments of the molecule. According to Equation (3) this energy can be split into three main components.

$$\Delta E_{\text{int}} = \Delta E_{\text{elstat}} + \Delta E_{\text{Pauli}} + \Delta E_{\text{orb}} \quad (3)$$

ΔE_{elstat} describes the classical Coulomb interaction between the fragments; ΔE_{Pauli} , which represents the exchange repulsion or Pauli repulsion, takes into account the destabilizing two-orbital three- or four-electron interactions between the occupied orbitals of both fragments, and ΔE_{orb} is the orbital interaction between the occupied and virtual orbitals of the two fragments. It has been suggested that the covalent and electrostatic character of the bond can be given by the ratio $\Delta E_{\text{elstat}}/\Delta E_{\text{orb}}$.^[42,43,57–60]

The electronic structures of the studied complexes were examined by NBO analysis.^[61] All MO pictures were made by using the MOLDEN program.^[62]

Results and Discussion

Geometries

Alkylborylene Complexes of Manganese and Rhenium

Herein we report the calculated structures of the manganese and rhenium alkylborylene complexes $[(\eta^5\text{-C}_5\text{H}_5)(\text{CO})_2\text{M}(\text{BR})]$ I–VIII. The important bond lengths and angles of the alkylborylene complexes I–VIII calculated at the BP86/TZ2P level of theory are presented in Table 1. The optimized geometries of manganese alkylborylene complexes $[(\eta^5\text{-C}_5\text{H}_5)(\text{CO})_2\text{Mn}(\text{BR})]$ I–IV are shown in Figure 2. The geometries of the rhenium alkylborylene complexes V–VIII are very similar to those presented in Figure 2, and therefore are not included into this figure.

Table 1. Selected optimized geometrical parameters for alkylborylene complexes $[(\eta^5\text{-C}_5\text{H}_5)(\text{CO})_2\text{M}(\text{BR})]$ (M = Mn, Re; R = Me, Et, *i*Pr, *t*Bu).^[a]

	$[(\eta^5\text{-C}_5\text{H}_5)(\text{CO})_2\text{Mn}(\text{BR})]$				$[(\eta^5\text{-C}_5\text{H}_5)(\text{CO})_2\text{Re}(\text{BR})]$			
	R = Me I	R = Et II	R = <i>i</i> Pr III	R = <i>t</i> Bu IV	R = Me V	R = Et VI	R = <i>i</i> Pr VII	R = <i>t</i> Bu VIII
Bond lengths								
M–B	1.786	1.787	1.788	1.790 [1.809(9)] ^[b]	1.938	1.939	1.939	1.940
B–C	1.544	1.548	1.553	1.560 [1.531(11)]	1.542	1.546	1.550	1.548
M–CO	1.773	1.773	1.771	1.771	1.915	1.916	1.914	1.915
C–O	1.168	1.169	1.169	1.169	1.169	1.169	1.169	1.169
Bond angles								
M–B–C	177.4	178.3	176.8	177.6 [174.3(7)]	179.9	179.2	179.7	179.9
B–M–CO	85.1	85.6	84.9	85.3	85.7	86.2	85.5	85.8
M–C–O	178.5	178.5	178.6	178.6	177.1	177.0	177.1	177.1
OC–M–CO	93.8	93.5	93.6	93.5	90.6	90.5	90.5	90.5

[a] Distances are given in Ångström and angles in degrees. [b] X-ray structure data for $[(\eta^5\text{-C}_5\text{H}_5)(\text{CO})_2\text{Mn}(\text{BrBu})]$.^[9]

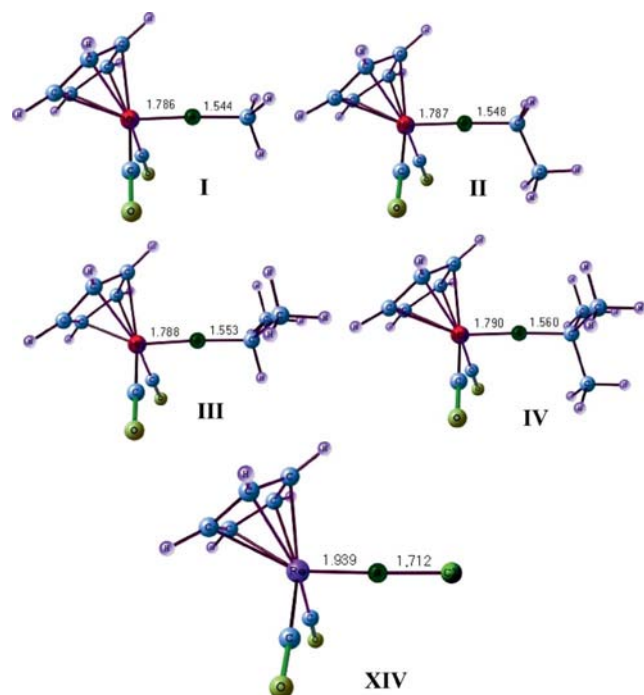


Figure 2. Optimized geometries of borylene complexes $[(\eta^5\text{-C}_5\text{H}_5)(\text{CO})_2\text{Mn}(\text{BR}_3)]$ (**I**, R = Me; **II**, R = Et; **III**, R = *i*Pr; **IV**, R = *t*Bu) and $[(\eta^5\text{-C}_5\text{H}_5)(\text{CO})_2\text{Re}(\text{BCl})]$ (**XIV**). The important bond lengths and angles are given in Table 1 and Table 2.

As shown in Table 1, the optimized bond lengths for Mn–B and B–C are in close agreement with the experimental values for **IV**.^[4] We expect the same accuracy for the other studied metal–borylene complexes of Mn and Re. The M–B bond lengths in the studied alkylborylene complexes **I–VIII** are shorter than those expected for M–B single bonds, based on predictions made from the sum of the covalent radii (Mn–B = 2.00 Å, Re–B = 2.15 Å).^[63] Using the relationship between bond order and bond length suggested by Pauling,^[64] the Pauling bond order of the optimized M–B bond lengths in these complexes are: 2.00 (**I**); 2.00 (**II**); 1.99 (**III**); 1.98 (**IV**); 1.99 (**V**); 1.98 (**VI**); 1.98 (**VII**);

1.98 (**VIII**). Thus, the M–B bonds in the complexes **I–VIII** are nearly M=B double bonds. The nature of the alkyl substituent in the borylenes BR has an insignificant effect on the character of M=BR bonding: the M=B bond length in complexes **I–VIII**, only slightly increases as R progresses from Me to *t*Bu; M=Mn: 1.786 Å (**I**), 1.787 Å (**II**), 1.788 Å (**III**), 1.790 Å (**IV**); M=Re: 1.938 Å (**V**), 1.939 Å (**VI**), 1.939 Å (**VII**), 1.940 Å (**VIII**).

The optimized B–C bond lengths, 1.542–1.560 Å, in complexes **I–VIII**, are slightly shorter than those expected for a single bond based on covalent radii predictions (B–C 1.59 Å).^[63] The M–B–C bond angles in the complexes deviate slightly from linearity due to some interaction of boron with CO or PMe_3 (Table 1).

Haloborylene Complexes of Manganese and Rhenium

The important bond lengths and angles of the haloborylene complexes **IX–XVI** calculated at the BP86/TZ2P level of theory are presented in Table 2. The optimized geometries of the rhenium chloroborylene complex $[(\eta^5\text{-C}_5\text{H}_5)(\text{CO})_2\text{Re}(\text{BCl})]$ **XIV** are shown in Figure 2. The geometries of the remaining haloborylene complexes of manganese and rhenium **IX–XIII**, **XV**, **XVI** are very similar to those presented in Figure 2, and therefore are not included.

The M–B bond lengths in the studied haloborylene complexes **IX–XVI** are also shorter than the M–B single bonds. Applying the aforementioned Pauling bond order criteria for the optimized M–B bond lengths results in the following Pauling bond orders 1.91 (**IX**); 1.98 (**X**); 1.96 (**XI**); 2.01 (**XII**); 1.92 (**XIII**); 1.98 (**XIX**); 1.98 (**XV**); 2.02 (**XVI**). Thus, similar to the alkylborylene species, the M–B bonds in the complexes **IX–XVI** are almost M=B double bonds. The optimized M=B bond lengths are shorter for X = I [1.784 Å, **XII** (M = Mn); 1.933 Å, **XVI** (M = Re)] and relatively longer for X = F [1.800 Å, **IX** (M = Mn); 1.949 Å, **X** (M = Re)]. The calculated M=B bond lengths are longer for haloborylene complexes than alkylborylene complexes (see Tables 1 and 2). The M–B–X bond angles of the haloborylene complexes again deviate slightly from linearity (Table 2).

Table 2. Selected optimized geometrical parameters for haloborylene complexes $[(\eta^5\text{-C}_5\text{H}_5)(\text{CO})_2\text{M}(\text{BX})]$ (M = Mn, Re; X = F, Cl, Br, I).^[a]

	$[(\eta^5\text{-C}_5\text{H}_5)(\text{CO})_2\text{Mn}(\text{BX})]$				$[(\eta^5\text{-C}_5\text{H}_5)(\text{CO})_2\text{Re}(\text{BX})]$			
	X = F IX	X = Cl X	X = Br XI	X = I XII	X = F XIII	X = Cl XIV	X = Br XV	X = I XVI
Bond lengths								
M–B	1.800	1.789	1.792	1.784	1.949	1.939	1.940	1.933
B–X	1.294	1.713	1.880	2.095	1.295	1.712	1.878	2.093
M–CO	1.776	1.777	1.778	1.779	1.918	1.919	1.919	1.920
C–O	1.166	1.166	1.165	1.165	1.167	1.167	1.166	1.166
Bond angles								
M–B–X	178.7	178.7	179.0	179.0	178.8	178.6	178.4	178.7
B–M–CO	87.9	85.1	87.5	87.2	87.4	87.0	87.3	87.1
M–C–O	178.5	178.5	178.4	178.4	176.8	177.0	176.7	176.8
OC–M–CO	93.1	93.3	93.3	93.3	90.5	90.4	90.4	90.4

[a] Distances are given in Ångström and angles in degrees.

In order to compare the nature of the bonding in fluoro-borylene (BF) complexes with those of isoelectronic CO and N₂ complexes, calculations have been performed for the complexes [(η⁵-C₅H₅)(CO)₂M(L)] (MnCO, M = Mn, L = CO; MnN₂, M = Mn, L = N₂; ReCO, M = Re, L = CO; ReN₂, M = Re, L = N₂) at the BP86/TZ2P level of theory and the important geometrical data are presented in Table 3.

Table 3. Selected optimized geometrical parameters for carbonyl and dinitrogen complexes [(η⁵-C₅H₅)(CO)₂M(L)] (M = Mn, Re; L = CO, N₂).^[a]

	[(η ⁵ -C ₅ H ₅)(CO) ₂ Mn(L)]		[(η ⁵ -C ₅ H ₅)(CO) ₂ Re(L)]	
	L = CO MnCO	L = N ₂ MnN ₂	L = CO ReCO	L = N ₂ ReN ₂
Bond lengths				
M–CO	1.783	1.783	1.921	1.916
C–O	1.163	1.164	1.165	1.167
M–N	–	1.837	–	1.961
N–N	–	1.123	–	1.127
Bond angles				
M–C–O	178.4	176.9	178.4	175.4
OC–M–CO	92.8	92.2	90.1	90.1
M–N–N	–	177.2	–	175.1
N–M–CO	–	94.4	–	91.9

[a] Distances are given in Ångström and angles in degrees.

Bonding Analysis of the M=BR and M=BX Bonds of the Complexes I–XII

In this section, the M=B bonding in borylene complexes I–XVI is analyzed, including a discussion of bond orders and atomic charges. The calculated Wiberg bond indices (WBI)^[65] and NPA charges are shown in Figure 3.

As seen from Figure 3, the WBI values of the M–B bonds for the alkylborylene [M = Mn: 1.08 (I), 1.07 (II), 1.05 (III), 1.01 (IV); M = Re: 1.34 (V), 1.33 (VI), 1.31 (VII), 1.27 (VIII)] and haloborylene complexes [M = Mn: 0.99 (IX), 1.05 (X), 1.06 (XI), 1.07 (XII); M = Re: 1.19 (XIII), 1.27 (XIV), 1.28 (XV), 1.30 (XVI)] were determined. One can infer from these observations that (1) the Re–B bonds are stronger than the corresponding Mn–B bonds in the studied complexes, (2) in alkylborylene complexes I–VIII, the strength of the M–B bonds decreases upon increasing substituent size (R = Me to *t*Bu) and (3) in haloborylene complexes IX–XVI, the strength of the M–B bonds increases as the halide group is descended (X = F to I) (i.e. M–B bonds are strongest for iodoborylene complexes). It is significant to note that the WBI values for M–B bonds are larger than those for the M–C bonds in corresponding carbonyl complexes. The results reveal that the BR/BX ligands in these borylene complexes are more strongly bound than the CO ligands.

The calculated natural population analysis (NPA) charge distributions indicate that the metal atoms carry negative charges, while the boron atoms carry significantly larger positive charges. The carbonyl groups are positively charged

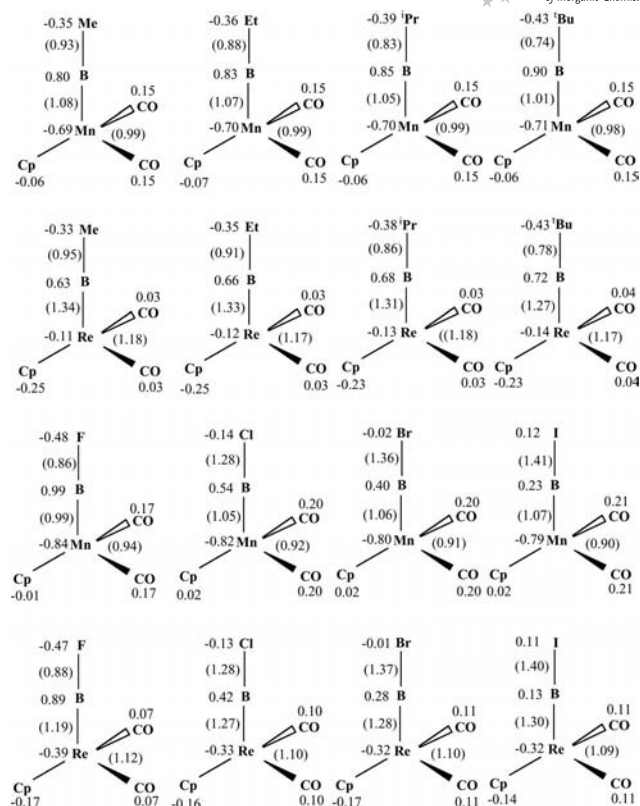


Figure 3. Wiberg bond indices (WBI) in parentheses and natural population analysis (NPA) charge distribution in terminal alkylborylene complexes [(η⁵-C₅H₅)(CO)₂M(BR)] and haloborylene complexes [(η⁵-C₅H₅)(CO)₂M(BX)] (M = Mn, Re; R = Me, Et, *i*Pr, *t*Bu; X = F, Cl, Br, I) (I–XVI).

in all studied borylene complexes. It is important to note that the difficulty in isolating transition metal alkyl- and haloborylene complexes is not caused by weak M–BR bonds, but rather by the high polarity of the metal-boron linkage and the build-up of positive charge at the boron center.

A more definitive picture of M=B bonding is obtained through NBO analysis of the delocalized Kohn–Sham orbitals. The results of the natural bond orbital (NBO) analysis (M–B, B–C and B–X σ bonds) are presented in Table 4. The M–B π bonding orbital is not observed in the NBO analysis of all the complexes under investigation (See Supporting Information). This indicates weaker M–B π bonding, which is significantly polarized towards the metal atom with the contributions of boron being very small. In most of the complexes I–XVI, the M–B σ bonding orbitals are slightly polarized towards the metal atom except for the haloborylene complexes of manganese [(η⁵-C₅H₅)(CO)₂Mn(BX)] IX–XII, where the M–B σ bonding orbitals are polarized towards the boron atom.

Energy Decomposition Analysis of the M=B Bonding of the Complexes I–XVI

Besides the charge decomposition analysis at the NBO level we also carried out an energy decomposition analysis

Table 4. Results of the NBO analysis of terminal alkylborylene complexes $[(\eta^5\text{-C}_5\text{H}_5)(\text{CO})_2\text{M}(\text{BR})]$ and haloborylene complexes $[(\eta^5\text{-C}_5\text{H}_5)(\text{CO})_2\text{M}(\text{BX})]$.

	$[(\eta^5\text{-C}_5\text{H}_5)(\text{CO})_2\text{Mn}(\text{BR})]$				$[(\eta^5\text{-C}_5\text{H}_5)(\text{CO})_2\text{Re}(\text{BR})]$				$[(\eta^5\text{-C}_5\text{H}_5)(\text{CO})_2\text{Mn}(\text{BX})]$				$[(\eta^5\text{-C}_5\text{H}_5)(\text{CO})_2\text{Mn}(\text{BX})]$			
R/X =	Me	Et	<i>i</i> Pr	<i>t</i> Bu	Me	Et	<i>i</i> Pr	<i>t</i> Bu	F	Cl	Br	I	F	Cl	Br	I
NBO bond analysis																
M–B σ bond																
Occupation	1.737	1.710	1.720	1.706	1.900	1.896	1.914	1.907	1.824	1.769	1.765	1.755	1.892	1.874	1.897	1.895
%M	54.08	54.16	54.04	54.27	55.14	55.10	53.16	53.15	47.80	48.61	48.30	48.08	54.58	53.78	53.70	53.55
%s	34.89	34.91	35.51	35.90	30.55	30.41	31.29	31.22	34.69	37.25	37.74	38.10	29.67	26.12	29.33	28.43
%p	0.08	0.09	0.11	0.15	0.04	0.05	0.06	0.07	0.06	0.06	0.07	0.06	0.07	0.06	0.05	0.05
%d	65.02	65.00	64.38	63.95	69.36	69.48	68.58	68.63	65.25	62.69	62.18	61.84	70.24	73.80	70.60	71.49
%f	0.01	0.01	0.00	0.00	0.05	0.06	0.07	0.08	0.01	0.00	0.01	0.00	0.02	0.02	0.02	0.03
%B	45.92	45.85	45.96	45.73	44.86	44.90	46.84	46.85	52.20	51.39	51.70	51.92	45.42	46.22	46.30	46.45
%s	54.85	54.34	54.15	53.94	47.04	46.42	51.78	51.27	81.58	65.31	64.39	63.59	61.29	53.81	53.36	52.62
%p	45.11	45.63	45.81	46.02	52.92	53.54	48.18	48.70	18.33	34.62	35.52	36.28	38.65	46.16	46.60	47.33
%d	0.03	0.02	0.03	0.03	0.03	0.03	0.03	0.02	0.08	0.07	0.08	0.12	0.06	0.02	0.04	0.05
%f	0.01	0.01	0.01	0.01	0.01	0.01	0.01	0.01	0.01	0.00	0.01	0.01	0.00	0.01	0.00	0.00
B–C/X σ bond																
Occupation	1.984	1.710	1.720	1.706	1.989	1.982	1.973	1.961	1.986	1.990	1.985	1.978	–	1.996	1.993	1.989
%B	28.85	54.16	54.04	54.27	29.81	29.16	28.37	27.11	–	27.73	32.67	40.02	–	28.83	33.99	40.91
%s	45.95	34.91	35.51	35.90	45.47	45.41	46.48	46.98	–	37.48	38.03	37.51	–	36.85	37.56	38.17
%p	54.01	0.09	0.11	0.15	54.49	54.54	53.45	52.95	–	62.11	61.84	61.97	–	62.71	62.14	61.60
%d	0.04	65.00	64.38	63.95	0.04	0.05	0.06	0.06	–	0.41	0.13	0.51	–	0.42	0.30	0.22
%f	0.00	0.01	0.00	0.00	0.00	0.01	0.01	0.01	–	0.00	0.00	0.01	–	0.02	0.00	0.01
									LP(F) ^[a]				LP(F) ^[b]			
%C/X	71.15	45.85	45.96	45.73	70.19	70.84	71.63	72.89	–	72.27	67.33	59.98	–	71.17	66.01	59.09
%s	33.98	54.34	54.15	53.94	33.80	32.02	29.77	26.83	50.09	34.72	28.18	22.34	–	34.03	27.59	22.01
%p	65.85	45.63	45.81	46.02	66.05	67.86	70.11	73.06	49.89	64.96	71.19	77.49	–	65.67	72.14	77.73
%d	0.16	0.02	0.03	0.03	0.13	0.12	0.11	0.11	0.02	0.32	0.61	0.16	–	0.29	0.27	0.26
%f	0.01	0.01	0.01	0.01	0.02	0.00	0.01	0.01	0.00	0.00	0.02	0.01	–	0.01	0.00	0.00

[a] Two lone-pairs on F: occupation 1.986, %s (50.09), %p (49.89), %d (0.02), %f (0.00) and occupation 1.722, %s (49.90), %p (50.00), %d (0.09), %f (0.00). [b] Two lone-pairs on F: occupation 1.987, %s (50.63), %p (49.35), %d (0.02), %f (0.00) and occupation 1.707, %s (49.36), %p (50.55), %d (0.09), %f (0.00).

of the M=B bonds in the calculated borylene complexes of manganese and rhenium $[(\eta^5\text{-C}_5\text{H}_5)(\text{CO})_2\text{M}(\text{BR})]$ (R = Me, Et, *i*Pr, *t*Bu) **I–VIII** and $[(\eta^5\text{-C}_5\text{H}_5)(\text{CO})_2\text{M}(\text{BX})]$ (X = F, Cl, Br, I) **IX–XVI**. The results are given in Table 5 and Figure 4.

The bond dissociation energies given in Table 5 and Figure 4 reveal the expected periodic trend in bond strengths due to d-orbital extent: the Re=B bonds are slightly stronger than the Mn=B bonds. Figure 4 shows a diagram of the π bonding, σ bonding, interaction energies ΔE_{int} , or-

Table 5. Energy decomposition analysis^[a] of terminal alkylborylene complexes $[(\eta^5\text{-C}_5\text{H}_5)(\text{CO})_2\text{M}(\text{BR})]$ and haloborylene complexes $[(\eta^5\text{-C}_5\text{H}_5)(\text{CO})_2\text{M}(\text{BX})]$.

	$[(\eta^5\text{-C}_5\text{H}_5)(\text{CO})_2\text{Mn}(\text{BR})]$				$[(\eta^5\text{-C}_5\text{H}_5)(\text{CO})_2\text{Re}(\text{BR})]$				$[(\eta^5\text{-C}_5\text{H}_5)(\text{CO})_2\text{Mn}(\text{BX})]$				$[(\eta^5\text{-C}_5\text{H}_5)(\text{CO})_2\text{Mn}(\text{BX})]$			
R/X =	Me	Et	<i>i</i> Pr	<i>t</i> Bu	Me	Et	<i>i</i> Pr	<i>t</i> Bu	F	Cl	Br	I	F	Cl	Br	I
ΔE_{int}	–107.6	–107.5	–107.4	–106.8	–127.1	–126.8	–126.9	–126.2	–81.5	–92.2	–92.6	–94.9	–99.6	–111.1	–111.6	–114.1
ΔE_{Pauli}	274.5	274.3	275.7	273.2	326.8	327.6	328.4	326.7	200.5	219.8	213.8	220.9	243.9	265.0	259.3	267.6
ΔE_{elstat}	–231.8	–232.1	–232.8	–230.3	–297.9	–299.0	–299.5	–297.4	–158.5	–173.5	–166.8	–170.2	–207.6	–226.0	–218.7	–223.5
^[b]	60.7%	60.8%	60.7%	60.6	65.6%	65.8%	65.8%	65.7%	56.2%	55.6%	54.4%	53.9%	60.4%	60.1%	58.9%	58.5%
ΔE_{orb}	–150.3	–149.7	–150.3	–149.7	–156.0	–155.4	–155.8	–155.5	–123.5	–138.5	–139.6	–145.7	–136.0	–150.2	–152.3	–158.2
$\Delta E_{\sigma}(\text{a}')$	–115.3	–115.4	–115.5	–115.3	–120.2	–120.3	–120.3	–120.4	–92.2	–103.1	–103.6	–108.1	–102.3	–112.7	–114.0	–118.2
$\Delta E_{\pi}(\text{a}'')$	–35.0	–34.3	–34.8	–34.4	–35.8	–35.1	–35.5	–35.2	–31.3	–35.4	–36.0	–37.6	–33.7	–37.5	–38.3	–40.0
^[c]	23.3%	22.9%	23.1%	23.0%	22.9%	22.6%	22.8%	22.6%	25.3%	25.6%	25.8%	25.8%	24.8%	25.0%	25.1%	25.3%
ΔE_{prep}	2.5	2.6	2.7	2.7	6.8	6.7	7.0	6.9	1.8	2.0	2.0	2.6	5.1	5.8	6.1	6.8
$\Delta E(-\text{BDE})^{\text{[d]}}$	–105.1	–104.9	–104.7	–104.1	–120.3	–120.1	–119.9	–119.3	–79.7	–90.2	–90.6	–92.3	–94.5	–105.3	–105.5	–107.3

[a] Energy contributions in kcal/mol. [b] Percentage contribution to the total electrostatic interactions reflecting the ionic character of the bond. [c] Percentage contribution of π bonding to the total orbital interactions ΔE_{orb} . [d] Bond dissociation energy with negative sign.

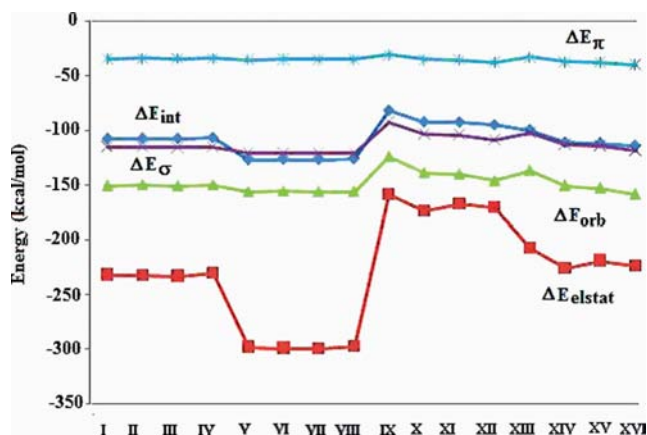


Figure 4. Values of the energy contributions of the interaction energies, π -bonding, σ -bonding, orbital interactions (covalent interactions) and electrostatic interactions (ionic contribution) to the M–B bonding in terminal alkylborylene complexes $[(\eta^5\text{-C}_5\text{H}_5)(\text{CO})_2\text{M}(\text{BR})]$ and haloborylene complexes $[(\eta^5\text{-C}_5\text{H}_5)(\text{CO})_2\text{M}(\text{BX})]$ (M = Mn, Re; R = Me, Et, *i*Pr, *t*Bu; X = F, Cl, Br, I) (I–XVI).

bital interaction energies ΔE_{orb} and electrostatic interactions ΔE_{elstat} . The breakdown of the interaction energy ΔE_{int} into the repulsive term ΔE_{Pauli} and the attractive terms ΔE_{orb} and ΔE_{elstat} shows that the ΔE_{Pauli} repulsive interaction has the larger absolute value for the studied complexes I–XVI (Table 5).

The question arises as to why the interaction energy, as well as the bond dissociation energy, of the Re=B bonds are greater than those of the Mn=B bonds. The variation in M=B bond energy depends on two factors: the metal center and the substituent at the boron atom. Upon changing the metal centre from manganese to rhenium, the absolute values of ΔE_{Pauli} , ΔE_{elstat} and ΔE_{orb} become larger, but for all the complexes studied, the sum of ΔE_{elstat} and ΔE_{orb} is found to be greater than that of the ΔE_{Pauli} . However, this difference is greater for rhenium borylene complexes than for manganese borylene complexes, resulting in higher interaction and bond dissociation energies for Re=B bonds than for Mn=B bonds.

The contributions of the electrostatic interaction terms ΔE_{elstat} are significantly larger in all borylene complexes I–XVI than the covalent bonding ΔE_{orb} term. Thus, the M=BR and M=BX bonds have a greater degree of ionic character (I–IV, Mn=BR: ca. 61.7%; V–VIII, Re=BR: ca. 65.7%; IX–XII, Mn=BX: 53.9–56.2%; XIII–XVI, Re=BX: 58.5–60.4%). The results reveal that: (1) the nature of the substituent R in BR has an insignificant effect on the ionic character of the M=BR bonds, while the ionic character of the M=BX bonds decreases as the halide group is descended (X = F to I) and (2) the ionic character in rhenium borylene complexes is greater than those in the corresponding manganese borylene complexes. These observations may be explained as (a) the net electron transfer from BX ligands to metal fragments $[(\eta^5\text{-C}_5\text{H}_5)(\text{CO})_2\text{M}]$ (Figure 3) decreases on going from X = F to X = I with concomitant decrease of ionic character, (b) the nature and proper-

ties of the HOMOs and LUMOs of the fragments $[(\eta^5\text{-C}_5\text{H}_5)(\text{CO})_2\text{M}]$ (M = Mn, Re), BR (R = Me, Et, *i*Pr, *t*Bu) and BX (X = F, Cl, Br, I) play a role in explaining the orbital interaction differences. The energies of the HOMOs and LUMOs of the metal fragments vary $\{[(\eta^5\text{-C}_5\text{H}_5)(\text{CO})_2\text{Mn}]$ (HOMO, –5.012 eV; –3.770 eV), $[(\eta^5\text{-C}_5\text{H}_5)(\text{CO})_2\text{Re}]$ (HOMO, –5.207 eV; –3.778 eV)}, while the energies of the HOMO and LUMO orbitals of the BR/BX fragments are: [BMe] (HOMO, –5.025 eV; –2.494 eV), [BEt] (HOMO, –4.902 eV; –2.365 eV), [BiPr] (HOMO, –4.827 eV; –2.413 eV), [BrBu] (HOMO, –4.783 eV; –2.338 eV) and [BF] (HOMO, –6.928 eV; –2.265 eV), [BCl] (HOMO, –6.403 eV; –3.013 eV), [BBR] (HOMO, –6.384 eV; –3.162 eV), [BCl] (HOMO, –6.272 eV; –3.385 eV). As a result, $[(\eta^5\text{-C}_5\text{H}_5)(\text{CO})_2\text{M}] \leftarrow \text{BX}$ σ -donation and $[(\eta^5\text{-C}_5\text{H}_5)(\text{CO})_2\text{M}] \rightarrow \text{BX}$ π -back donation increase upon going from X = F to X = I and from M = Mn to Re. As the orbital contribution to a bond increases, the ionic character decreases relatively. Table 5 also gives the breakdown of the orbital interactions ΔE_{orb} into the M \leftarrow BR σ donation and M \rightarrow BR π back-donation components. It is significant to note that the π bonding contribution in all complexes is smaller (22.6–25.8% of total orbital contributions) than the σ bonding contribution. Similar results have been reported earlier for terminal borylene complexes.^[39,40,43,44] A larger π contribution is found for the haloborylene complexes $[(\eta^5\text{-C}_5\text{H}_5)(\text{CO})_2\text{M}(\text{BX})]$ (IX–XVI) than for the alkylborylene complexes $[(\eta^5\text{-C}_5\text{H}_5)(\text{CO})_2\text{M}(\text{BR})]$ (I–VIII). From the data presented in Table 5 it could be concluded that: (1) in the BR and BX ligands, boron predominantly behaves as a σ donor, (2) the bond dissociation energy is higher for Re than Mn, and (3) the interaction energy is lowest for fluoroborylene complexes $[(\eta^5\text{-C}_5\text{H}_5)(\text{CO})_2\text{M}(\text{BF})]$ (M = Mn, Re).

We wish to emphasize that the calculated energy contribution ΔE_{π} gives only the out-of-plane (π_{\perp}) component of the M \rightarrow BR π back-donation, which is schematically shown in Figure 1. This is because the molecules have C_s symmetry and thus the orbitals can only have $a'(\sigma)$ or $a''(\pi)$ symmetry. Thus, the energy contributions of the $a'(\sigma)$ orbitals come from the M \leftarrow BR σ donation but also from the in-plane M \rightarrow BR π back-donation. For molecules with C_s symmetry, it is not possible to separate the later two interactions due to the orbitals, a' symmetry.

Via computation, we have theoretically examined the bonding situation in the transition metal haloborylene, carbonyl and dinitrogen complexes using energy decomposition analysis. Table 6 shows the calculated bond energies of the $[(\eta^5\text{-C}_5\text{H}_5)(\text{CO})_2\text{M}]\text{-CO}$ and $[(\eta^5\text{-C}_5\text{H}_5)(\text{CO})_2\text{M}]\text{-N}_2$ bonds and the energy decomposition into terms comprising Pauli repulsion, orbital interaction and electrostatic interaction. The calculations reveal that the metal-ligand bond dissociation energies increase in the order $\text{N}_2 < \text{CO} < \text{BF}$, indicating that borylene ligands are more strongly bound than the isoelectronic CO and N_2 ligands.

Surprisingly, comparison of the bonding contributions to the $[(\eta^5\text{-C}_5\text{H}_5)(\text{CO})_2\text{M}]\text{-CO}$ and $[(\eta^5\text{-C}_5\text{H}_5)(\text{CO})_2\text{M}]\text{-BF}$ bonds showed the π -bonding contributions of the CO and

Table 6. Energy decomposition analysis of carbonyl and dinitrogen complexes $[(\eta^5\text{-C}_5\text{H}_5)(\text{CO})_2\text{M}(\text{L})]$ ($\text{M} = \text{Mn, Re}$; $\text{L} = \text{CO, N}_2$).^[a]

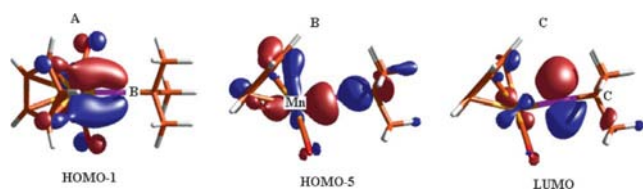
	$[(\eta^5\text{-C}_5\text{H}_5)(\text{CO})_2\text{Mn}(\text{L})]$		$[(\eta^5\text{-C}_5\text{H}_5)(\text{CO})_2\text{Re}(\text{L})]$	
	$\text{L} = \text{CO}$	$\text{L} = \text{N}_2$	$\text{L} = \text{CO}$	$\text{L} = \text{N}_2$
	MnCO	MnN₂	ReCO	ReN₂
ΔE_{int}	−62.7	−37.2	−77.5	−44.3
ΔE_{Pauli}	144.3	86.4	191.0	123.8
ΔE_{elstat}	−105.1	−55.4	−142.9	−78.1
[b]	50.8%	44.8%	53.2%	46.5%
ΔE_{orb}	−101.9	−68.2	−125.6	−90.0
$\Delta E_{\sigma}(\text{a}')$	−70.6	−46.5	−89.8	−64.3
$\Delta E_{\pi}(\text{a}'')$	−31.3	−21.7	−35.8	−25.7
[c]	30.7%	31.8%	28.5%	28.6%
ΔE_{prep}	2.0	1.5	4.9	3.0
$\Delta E(-\text{BDE})$ ^[d]	−60.7	−35.7	−72.6	−41.3

[a] Energy contributions in kcal/mol. [b] Percentage contribution to the total electrostatic interactions reflecting the ionic character of the bond. [c] Percentage contribution of π bonding to the total orbital interactions ΔE_{orb} . [d] Bond dissociation energy with negative sign.

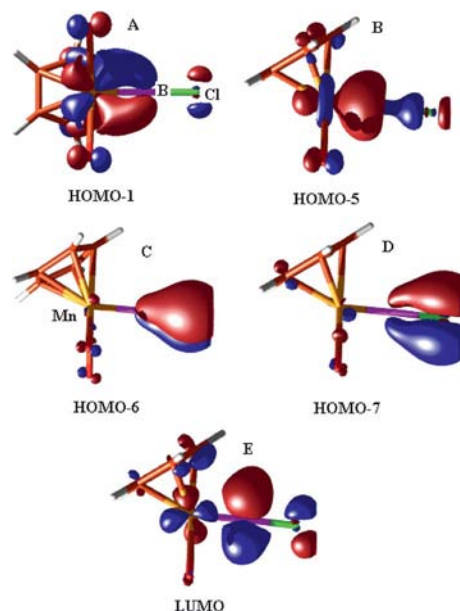
BF ligands to be almost the same (see Tables 5 and 6). However, their contribution to the σ -bonding is clearly the dominating term of the orbital interaction energy for the $[(\eta^5\text{-C}_5\text{H}_5)(\text{CO})_2\text{M}]\text{-BX}$ bonds. This may be explained by considering the energy levels of the frontier orbitals of CO (5σ , −9.125 eV; 2π , −2.082 eV) and BF (5σ , −6.928 eV; 2π , −2.265 eV). The energy of the 5σ HOMO of BF is much higher than that of CO, while the energy of the 2π LUMO of BF is slightly lower in energy than the corresponding CO 2π orbital. This explains why the π -bonding energy values for the BF and CO ligands in the complexes $[(\eta^5\text{-C}_5\text{H}_5)(\text{CO})_2\text{M}]\text{-BF}$ and $[(\eta^5\text{-C}_5\text{H}_5)(\text{CO})_2\text{M}]\text{-CO}$ change very little.

The low-lying HOMO (−10.234 eV) of N_2 suggests that the metal– N_2 bond dissociation energy of dinitrogen complexes $[(\eta^5\text{-C}_5\text{H}_5)(\text{CO})_2\text{M}]\text{-N}_2$ ($\text{M} = \text{Mn, Re}$) should be lower than the bond dissociation energy of the CO and BX ligands, and this is indeed the case. The calculated bond energy of $[(\eta^5\text{-C}_5\text{H}_5)(\text{CO})_2\text{M}]\text{-N}_2$ is significantly lower than the BDEs of $[(\eta^5\text{-C}_5\text{H}_5)(\text{CO})_2\text{M}]\text{-CO}$ and $[(\eta^5\text{-C}_5\text{H}_5)(\text{CO})_2\text{M}]\text{-BF}$ (see Tables 5 and 6).

To visualize the M–B bonding in alkylborylene complexes, envelope plots of some relevant orbitals of the manganese complex $[(\eta^5\text{-C}_5\text{H}_5)(\text{CO})_2\text{Mn}(\text{B}t\text{Bu})]$ (**IV**) are given in Figure 5. The HOMO-1 (Figure 5, A) gives an unmistakable pictorial description of the $\text{Mn}=\text{B}$ π bonding, the HOMO-5 (Figure 5, B) shows $\text{Mn}=\text{B}$ σ bonding, while the LUMO (Figure 5, C) is a B π orbital. To visualize the M–B and B–X bonding (see Figure 1) in haloborylene complexes,

Figure 5. Plot of some relevant orbitals of the manganese alkylborylene complex $[(\eta^5\text{-C}_5\text{H}_5)(\text{CO})_2\text{Mn}(\text{B}t\text{Bu})]$ (**IV**).

plots of some relevant orbitals of the complex $[(\eta^5\text{-C}_5\text{H}_5)(\text{CO})_2\text{Mn}(\text{BCl})]$ (**X**) are given in Figure 6. The HOMO-1 (Figure 6, A) is a $\text{Mn}=\text{B}$ π orbital, while the HOMO-5 (Figure 6, B) shows mainly the $\text{Mn}=\text{B}$ σ bonding orbital. The LUMO (Figure 6, E) is mainly a non-bonding p_π orbital at B. The HOMO-6 (Figure 6, C) and HOMO-7 (Figure 6, D) are B–Cl π orbitals.

Figure 6. Plot of some relevant orbitals of the manganese chloroborylene complex $[(\eta^5\text{-C}_5\text{H}_5)(\text{CO})_2\text{Mn}(\text{BCl})]$ (**X**).

Mechanism for the Reaction of the Bridging Borylene Complex $[\{(\eta^5\text{-C}_5\text{H}_5)(\text{CO})_2\text{Mn}\}_2(\mu\text{-BCl})]$ with CO

In 2002 it was observed that the bridged chloroborylene complex $[(\eta^5\text{-C}_5\text{H}_5)(\text{CO})_2\text{Mn}(\text{BCl})]$, upon photolysis, gave the unusual metallaborane species $[\{(\eta^5\text{-C}_5\text{H}_5)(\text{CO})_2\text{Mn}\}_2(\eta^1\eta^1\text{-}\mu\text{-B}_2\text{Cl}_2)]$ (**XX**) in yields of about 37%.^[34] At the time, it was proposed that the latter represents the formal dimerization product of the elusive terminal chloroborylene complex $[(\eta^5\text{-C}_5\text{H}_5)(\text{CO})_2\text{Mn}(\text{BCl})]$.^[34] In order to rationalize the formation of this metallaborane $[\{(\eta^5\text{-C}_5\text{H}_5)(\text{CO})_2\text{Mn}\}_2(\eta^1\eta^1\text{-}\mu\text{-B}_2\text{Cl}_2)]$ from the terminal borylene intermediate $[(\eta^5\text{-C}_5\text{H}_5)(\text{CO})_2\text{Mn}(\text{BCl})]$, the energy barrier for the dimerization process has been estimated at the BP86/TZ2P level with Zora relativistic correction. The important optimized geometrical parameters for compounds $[\{(\eta^5\text{-C}_5\text{H}_5)(\text{CO})_2\text{Mn}\}_2(\mu\text{-BCl})]$ (**XVII**), $[\{(\eta^5\text{-C}_5\text{H}_5)(\text{CO})_2\text{Mn}\}_2(\mu\text{-BCl})(\mu\text{-CO})]$ (**XVIII**), $[\{(\eta^5\text{-C}_5\text{H}_5)(\text{CO})_2\text{Mn}\}_2(\mu\text{-BCl})_2]$ (**TS**) (**XIX**) and $[\{(\eta^5\text{-C}_5\text{H}_5)(\text{CO})_2\text{Mn}\}_2(\eta^1\eta^1\text{-}\mu\text{-B}_2\text{Cl}_2)]$ (**XX**) are presented in Table 7 and structures are shown in Figure 7. The geometry of the compound **XX** is consistent with the experimental X-ray data.^[34] Figures 8 and 9 show the energy profiles of the reaction process.

The reaction of CO with the bridged borylene complex $[\{(\eta^5\text{-C}_5\text{H}_5)(\text{CO})_2\text{Mn}\}_2(\mu\text{-BCl})]$ spontaneously leads to formation of the intermediate complex $[\{(\eta^5\text{-C}_5\text{H}_5)(\text{CO})_2\text{Mn}\}_2(\mu\text{-BCl})(\mu\text{-CO})]$.

Table 7. Selected optimized geometrical parameters for bridged borylene complexes $[(\eta^5\text{-C}_5\text{H}_5)(\text{CO})_2\text{Mn}\}_2(\mu\text{-BCl})]$ (**XVII**), $[(\eta^5\text{-C}_5\text{H}_5)(\text{CO})_2\text{Mn}\}_2(\mu\text{-BCl})(\mu\text{-CO})]$ (**XVIII**), $[(\eta^5\text{-C}_5\text{H}_5)(\text{CO})_2\text{Mn}\}_2(\mu\text{-BCl})_2]$ (**XIX**) (TS) and $[(\eta^5\text{-C}_5\text{H}_5)(\text{CO})_2\text{Mn}\}_2(\eta\text{-}\eta\text{-}\mu\text{-B}_2\text{Cl}_2)]$ (**XX**).

	XVII	XVIII	XIX	XX
Bond lengths [Å]				
Mn–B	2.080	2.055	2.069	2.076
B–Cl	1.796	1.823	1.813	1.810
B–B	–	–	2.155	1.702
Mn–Mn	3.210	3.641	3.532	3.664
Mn–CO (terminal)	1.789	1.771	1.774	1.775
C–O (terminal)	1.164	1.165	1.166	1.165
Mn–CO (bridged)	–	2.089	–	–
C–O (bridged)	–	1.215	–	–
Bond angles [°]				
Mn–B–Cl	129.5	117.3	120.5	117.9
Mn–B–Mn	101.9	124.7	117.2	123.9
B–B–Cl	–	–	–	145.5
B–Mn–B	–	–	62.8	48.4

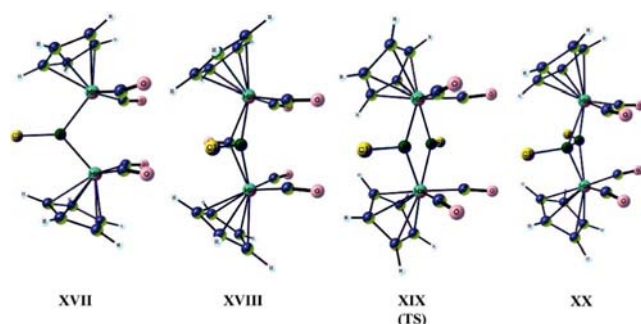


Figure 7. Optimized geometries of bridged borylene complexes $[(\eta^5\text{-C}_5\text{H}_5)(\text{CO})_2\text{Mn}\}_2(\mu\text{-BCl})]$ (**XVII**), $[(\eta^5\text{-C}_5\text{H}_5)(\text{CO})_2\text{Mn}\}_2(\mu\text{-BCl})(\mu\text{-CO})]$ (**XVIII**), $[(\eta^5\text{-C}_5\text{H}_5)(\text{CO})_2\text{Mn}\}_2(\mu\text{-BCl})_2]$ (**XIX**) (TS) and $[(\eta^5\text{-C}_5\text{H}_5)(\text{CO})_2\text{Mn}\}_2(\eta\text{-}\eta\text{-}\mu\text{-B}_2\text{Cl}_2)]$ (**XX**).

$\text{Mn}\}_2(\mu\text{-BCl})(\mu\text{-CO})]$ (**XVIII**) without any energetic barrier. The stabilization energy of the complex **XVIII** is 45.24 kcal/mol lower than that of the reactants **XVII** and CO. The dissociation of this intermediate complex **XVIII** into the manganese carbonyl complex $[(\eta^5\text{-C}_5\text{H}_5)\text{Mn}(\text{CO})_3]$ and the terminal borylene complex $[(\eta^5\text{-C}_5\text{H}_5)(\text{CO})_2\text{Mn}(\text{BCl})]$ also constitutes a strong exothermic process. An alternative pathway for the formation of the manganese carbonyl complex $[(\eta^5\text{-C}_5\text{H}_5)\text{Mn}(\text{CO})_3]$ and the terminal borylene complex $[(\eta^5\text{-C}_5\text{H}_5)(\text{CO})_2\text{Mn}(\text{BCl})]$ from the reaction of **XVII** and CO has also been investigated. The stabilization energy of the intermediate carbonyl-bridged complex $[(\eta^5\text{-C}_5\text{H}_5)(\text{CO})_2\text{Mn}\}_2(\mu\text{-CO})_2]$ and the terminal borylene complex $[(\eta^5\text{-C}_5\text{H}_5)(\text{CO})_2\text{Mn}(\text{BCl})]$ is 31.11 kcal/mol lower than that of the reactants **XVII** and CO. One may infer from these observations that the second pathway is less favorable than the first pathway, i.e. with formation of the intermediate complex **XVIII**, displaying both bridging BCl and CO ligands.

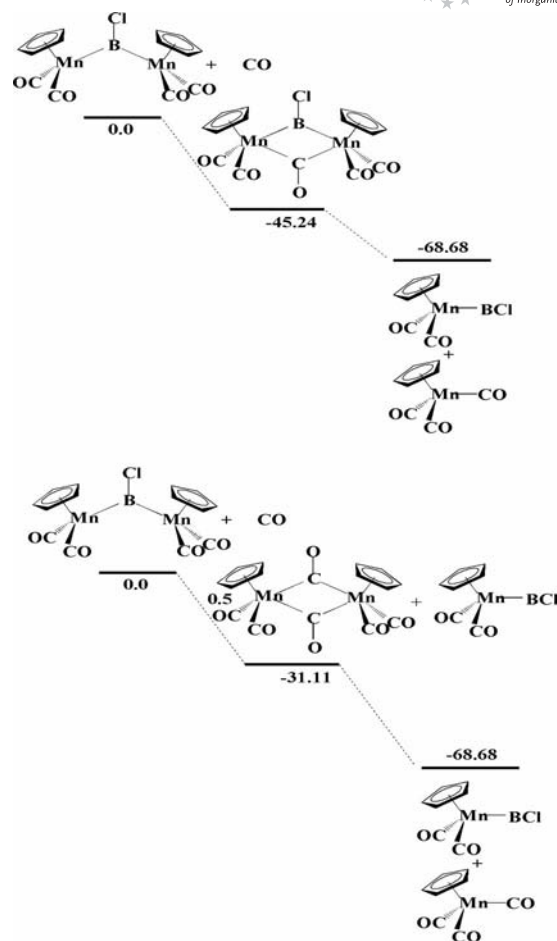


Figure 8. Two alternative reaction pathways for the preparation of $[(\eta^5\text{-C}_5\text{H}_5)(\text{CO})_2\text{Mn}(\text{BCl})]$ (**X**) and $[(\eta^5\text{-C}_5\text{H}_5)\text{Mn}(\text{CO})_3]$ (**MnCO**) from the reaction of the bridged borylene complex $[(\eta^5\text{-C}_5\text{H}_5)(\text{CO})_2\text{Mn}\}_2(\mu\text{-BCl})]$ (**XVII**) and CO. The energies are in kcal/mol. For the geometry of these structures, see Figure 7 and Table 7.

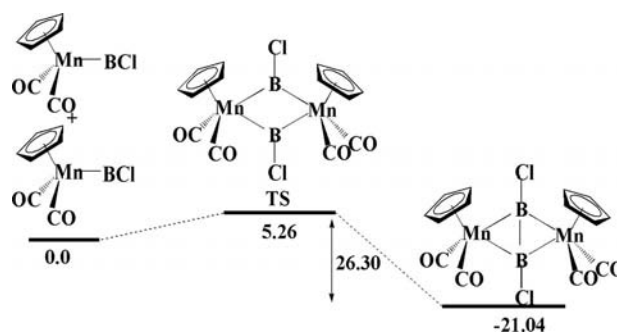


Figure 9. Reaction profile for the synthesis of the bridged system $[(\eta^5\text{-C}_5\text{H}_5)(\text{CO})_2\text{Mn}\}_2(\eta\text{-}\eta\text{-}\mu\text{-B}_2\text{Cl}_2)]$ (**XX**) from mononuclear terminal borylene complexes $[(\eta^5\text{-C}_5\text{H}_5)(\text{CO})_2\text{Mn}(\text{BCl})]$ (**X**). The energies are in kcal/mol. For the geometry of these structures, see Figure 7 and Table 7.

The theoretical calculations indicate a single-step mechanism for the dimerization of $[(\eta^5\text{-C}_5\text{H}_5)(\text{CO})_2\text{Mn}(\text{BCl})]$, involving a bridged bis(borylene) species $[(\eta^5\text{-C}_5\text{H}_5)(\text{CO})_2\text{-}$

$\text{Mn}\}_2(\mu\text{-BCl})_2]$ (TS/XIX). The B–B bond length (2.115 Å) of the transition state species XIX is significantly longer than that of the final product $[(\eta^5\text{-C}_5\text{H}_5)(\text{CO})_2\text{Mn}\}_2(\eta:\eta:\mu\text{-B}_2\text{Cl}_2)]$ (1.702 Å). The calculated barrier is relatively low (5.26 kcal/mol above the starting terminal borylene intermediate), which would favor fast dimerization. The formation of $[(\eta^5\text{-C}_5\text{H}_5)(\text{CO})_2\text{Mn}\}_2(\eta:\eta:\mu\text{-B}_2\text{Cl}_2)]$ from TS is an exothermic process (21.04 kcal/mol below the starting monomers) and the energies are clearly in favor of a dimerization reaction.

Conclusions

From the presented theoretical studies of the structure and bonding in 16 neutral borylene complexes of manganese and rhenium, one can draw the following conclusions: (1) For the first time (except in the case of complex IV), the geometry and electronic structure of $\text{M}=\text{BR}$ and $\text{M}=\text{BX}$ bonds in the neutral terminal alkylborylene and haloborylene complexes of manganese and rhenium $[(\eta^5\text{-C}_5\text{H}_5)(\text{CO})_2\text{M}(\text{BR})]$, $[(\eta^5\text{-C}_5\text{H}_5)(\text{CO})_2\text{M}(\text{BX})]$ ($\text{M} = \text{Mn, Re}$; $\text{R} = \text{Me, Et, } i\text{Pr, } t\text{Bu}$; $\text{X} = \text{F, Cl, Br, I}$) have been reported. The calculated geometry of the manganese borylene complex IV is in excellent agreement with the experimentally determined structure of $[(\eta^5\text{-C}_5\text{H}_5)(\text{CO})_2\text{Mn}(\text{BrBu})]$.^[4]

(2) The M–B bonds in the complexes I–XVI are almost $\text{M}=\text{B}$ double bonds, in which the σ bonding orbitals (except in the haloborylene complexes of manganese IX–XII) are *slightly* polarized towards the metal atom, and the π bonding orbital is *highly* polarized towards the metal atom. In all studied metal borylene complexes I–XVI, the π bonding contribution to the total $\text{M}=\text{B}$ bond is smaller than that of the σ bonding. The calculated energy contribution ΔE_π gives only the out-of-plane (π_\perp) component of the $[(\eta^5\text{-C}_5\text{H}_5)(\text{CO})_2\text{M}] \rightarrow \text{BR}$ π back-donation, which is schematically shown in Figure 1. This is because the molecules have C_s symmetry and thus the orbitals can only have the $a'(\sigma)$ or $a''(\pi)$ symmetry. Thus, the energy contributions of the $a'(\sigma)$ orbitals come from the $[(\eta^5\text{-C}_5\text{H}_5)(\text{CO})_2\text{M}] \leftarrow \text{BR}$ σ donation but also from the in-plane $[(\eta^5\text{-C}_5\text{H}_5)(\text{CO})_2\text{M}] \rightarrow \text{BR}$ π back-donation.

(3) The nature of the alkyl substituent has an insignificant effect on the character of $\text{M}=\text{BR}$ bonding: the $\text{M}=\text{B}$ bond lengths in complexes I–VIII only marginally increase as R progresses from Me to *t*Bu. In dramatic contrast, changing the substituent X in the haloborylene complexes IX–XVI from lighter to heavier halides results in stronger M–B bonds (shorter bond lengths, higher bond energies, higher WBI values). Both the σ and π contributions to the M–B bond energy were found to significantly increase as the halide becomes heavier, albeit the former increase has a greater impact on the bond stability. Along the same series ($\text{X} = \text{F} \rightarrow \text{I}$), the NPA charges on the X substituent become much less negative, and those on B become much less posi-

tive, i.e. the B–X bond becomes less ionic in character. The overall picture is that upon progressing from $\text{X} = \text{F}$ to $\text{X} = \text{I}$, the halide substituent promotes greater σ and π M–B bonding by becoming less σ -withdrawing from, as well as less π -donating to, the boron atom. Qualitatively, the former can be rationalized by the decreasing electronegativities of the heavier halides, while the latter can be partly attributed to increasing mis-match of the π -orbitals of B and X, leading to poor orbital overlap.

(4) The calculated WBI values for M–B bonds are slightly larger than those of M–CO bonds; that is, M–B bonds in these alkyl- and haloborylene complexes are stronger than M–CO bonds.

(5) The contributions of the electrostatic interactions ΔE_{elstat} are in all calculated borylene complexes I–XVI significantly larger than the covalent bonding ΔE_{orb} , that is, the $\text{M}=\text{BR}$ bonding in the borylene complexes has a greater degree of ionic character (ca. 61.7% for the complexes I–IV, ca. 65.7% for the complexes V–VIII, 53.9–56.2% for the complexes IX–XII and 58.5–60.4% for the complexes XIII–XVI). It should be noted that the π -bonding contribution in all complexes is smaller (22.6–25.8% of total orbital contributions) than the σ bonding contribution.

(6) While the formation of $[(\eta^5\text{-C}_5\text{H}_5)(\text{CO})_2\text{Mn}(\text{BCl})]$ from the bridging chloroborylene complex $[(\eta^5\text{-C}_5\text{H}_5)(\text{CO})_2\text{Mn}\}_2(\mu\text{-BCl})]$ was calculated to be strongly exothermic and barrierless, calculations suggest two alternative pathways for the process. The two possible dinuclear transition states, one with two bridging carbonyl ligands [i.e. “ $(\mu\text{-CO})_2$ ”] and a second with bridging carbonyl and chloroborylene ligands [i.e. “ $(\mu\text{-BCl})(\mu\text{-CO})$ ”] are separated by approximately 14 kcal/mol, thus we favour the latter as the predominant transition state. The dimerization step of the terminal borylene complex $[(\eta^5\text{-C}_5\text{H}_5)(\text{CO})_2\text{Mn}(\text{BCl})]$ to $[(\eta^5\text{-C}_5\text{H}_5)(\text{CO})_2\text{Mn}\}_2(\eta:\eta:\mu\text{-B}_2\text{Cl}_2)]$ is likewise a strongly exothermic process (21.04 kcal/mol below the starting monomers), operating via a small activation barrier involving formation of a transition state with two bridging borylene ligands [i.e. “ $(\mu\text{-BCl})_2$ ”] which combine to form the product.

We believe that a more detailed understanding of the bonding in metal-borylene complexes is a requisite, particularly for the synthesis of terminal transition metal borylene complexes and the design of efficient borylene transfer processes. While we know from experiment that, although decreasing the size of the alkyl group from *tert*-butyl has a detrimental effect on the *kinetic* stability of the complexes, these calculations show that this has little effect on their *thermodynamic* stability. Thus, terminal alkyl borylene complexes containing smaller alkyl substituents may be attainable if secondary sources of steric protection are used (e.g. bulky face-capping ligands). These calculations additionally point towards the possible synthesis of complexes containing the higher halides as borylene substituents by using a similar strategy.

Supporting Information (see footnote on the first page of this article): Cartesian coordinates of the optimised geometries of alkylborylene and haloborylene complexes I–XVI (PDF) and NBO bond analysis of M–B π bond observed in selected complexes.

Acknowledgments

K. K. P. gratefully acknowledges the Alexander von Humboldt Foundation, Germany for a fellowship.

- [1] a) E. O. Fischer, A. Maasböl, *Chem. Ber.* **1967**, *100*, 2445; b) E. O. Fischer, G. Besl, *Z. Naturforsch., Teil B* **1979**, *34*, 1186.
- [2] a) W. A. Herrmann, B. Reiter, H. Biersack, *J. Organomet. Chem.* **1975**, *97*, 245; b) S. Mock, U. Schubert, *Chem. Ber.* **1993**, *126*, 2591; c) B. Schiemenz, G. Huttner, *Chem. Ber.* **1994**, *127*, 2129.
- [3] H. Braunschweig, T. Wagner, *Angew. Chem.* **1995**, *107*, 904; *Angew. Chem. Int. Ed. Engl.* **1995**, *34*, 825.
- [4] H. Braunschweig, M. Burzler, T. Kupfer, K. Radacki, F. Seeler, *Angew. Chem.* **2007**, *119*, 7932; *Angew. Chem. Int. Ed.* **2007**, *46*, 7785.
- [5] H. Braunschweig, C. Kollan, U. Englert, *Angew. Chem.* **1998**, *110*, 3355; *Angew. Chem. Int. Ed.* **1998**, *37*, 3179.
- [6] A. H. Cowley, V. Lomeli, A. Voigt, *J. Am. Chem. Soc.* **1998**, *120*, 6401.
- [7] H. Braunschweig, M. Colling, C. Kollann, H. G. Stammer, B. Neumann, *Angew. Chem.* **2001**, *113*, 2359; *Angew. Chem. Int. Ed.* **2001**, *40*, 2298.
- [8] H. Braunschweig, M. Colling, C. Kollann, K. Merz, K. Radacki, *Angew. Chem.* **2001**, *113*, 4327; *Angew. Chem. Int. Ed.* **2001**, *40*, 4198.
- [9] H. Braunschweig, M. Colling, C. Hu, K. Radacki, *Angew. Chem.* **2003**, *115*, 215; *Angew. Chem. Int. Ed.* **2003**, *42*, 205.
- [10] H. Braunschweig, K. Radacki, D. Rais, K. Uttinger, *Angew. Chem.* **2006**, *118*, 169; *Angew. Chem. Int. Ed.* **2006**, *45*, 162.
- [11] H. Braunschweig, K. Radacki, D. Rais, K. Uttinger, *Organometallics* **2006**, *25*, 5159.
- [12] B. Blank, M. Colling-Hendelkens, C. Kollann, K. Radacki, D. Rais, K. Uttinger, G. R. Whittell, H. Braunschweig, *Chem. Eur. J.* **2007**, *13*, 4770.
- [13] H. Braunschweig, M. Forster, T. Kupfer, F. Seeler, *Angew. Chem.* **2008**, *120*, 6070; *Angew. Chem. Int. Ed.* **2008**, *47*, 5981.
- [14] G. Alcaraz, U. Helmstedt, E. Clot, L. Vendier, S. Sabo-Etienne, *J. Am. Chem. Soc.* **2008**, *130*, 12878.
- [15] D. L. Coombs, S. Aldridge, C. Jones, D. J. Willock, *J. Am. Chem. Soc.* **2003**, *125*, 6356.
- [16] D. L. Coombs, S. Aldridge, A. Rossin, C. Jones, D. J. Willock, *Organometallics* **2004**, *23*, 2911.
- [17] S. Aldridge, C. Jones, T. Gans-Eichler, A. Stasch, D. L. Kays, N. D. Coombs, D. J. Willock, *Angew. Chem.* **2006**, *118*, 6264; *Angew. Chem. Int. Ed.* **2006**, *45*, 6118.
- [18] D. Vidovic, M. Findlater, G. Reeske, H. Cowley, *Chem. Commun.* **2006**, 3786.
- [19] H. Braunschweig, K. Radacki, K. Uttinger, *Angew. Chem.* **2007**, *119*, 4054; *Angew. Chem. Int. Ed.* **2007**, *46*, 3979.
- [20] G. A. Pierce, D. Vidovic, D. L. Kays, N. D. Coombs, A. L. Thompson, E. D. Jemmis, S. De, S. Aldridge, *Organometallics* **2009**, *28*, 2947.
- [21] S. De, G. A. Pierce, D. Vidovic, D. L. Kays, N. D. Coombs, E. D. Jemmis, S. Aldridge, *Organometallics* **2009**, *28*, 2961.
- [22] D. A. Addy, G. A. Pierce, D. Vidovic, D. Mallick, E. D. Jemmis, J. M. Goicoechea, S. Aldridge, *J. Am. Chem. Soc.* **2010**, *132*, 4586.
- [23] H. Braunschweig, M. Colling, *J. Organomet. Chem.* **2000**, *614*–615, 18.
- [24] H. Braunschweig, *Adv. Organomet. Chem.* **2004**, *51*, 163.
- [25] H. Braunschweig, M. Colling, *Eur. J. Inorg. Chem.* **2003**, 393.
- [26] H. Braunschweig, D. Rais, *Heteroat. Chem.* **2005**, *16*, 566.
- [27] H. Braunschweig, C. Kollann, D. Rais, *Angew. Chem.* **2006**, *118*, 5380; *Angew. Chem. Int. Ed.* **2006**, *45*, 5254.
- [28] H. Braunschweig, C. Kollann, F. Seeler, *Struct. Bonding (Berlin)* **2008**, *130*, 1.
- [29] H. Braunschweig, R. D. Dewhurst, *Angew. Chem.* **2009**, *121*, 1925; *Angew. Chem. Int. Ed.* **2009**, *48*, 1893.
- [30] S. Aldridge, D. L. Coombs, *Coord. Chem. Rev.* **2004**, *248*, 535.
- [31] S. Aldridge, D. L. Kays, *Main Group Chem.* **2006**, *5*, 223.
- [32] D. Vidovic, G. A. Pierce, A. Aldridge, *Chem. Commun.* **2009**, 1157.
- [33] H. Braunschweig, R. D. Dewhurst, A. Schneider, *Chem. Rev.* **2010**, *110*, 3924.
- [34] H. Braunschweig, M. Colling, C. Hu, K. Radacki, *Angew. Chem.* **2002**, *114*, 1415; *Angew. Chem. Int. Ed.* **2002**, *41*, 1359.
- [35] A. W. Ehlers, E. J. Baerends, F. M. Bickelhaupt, U. Radius, *Chem. Eur. J.* **1998**, *4*, 210.
- [36] U. Radius, F. M. Bickelhaupt, A. W. Ehlers, N. Goldberg, R. Hoffmann, *Inorg. Chem.* **1998**, *37*, 1080.
- [37] C. L. B. Macdonald, A. H. Cowley, *J. Am. Chem. Soc.* **1999**, *121*, 12113.
- [38] C. Boehme, G. Frenking, *Chem. Eur. J.* **1999**, *5*, 2184.
- [39] J. Uddin, C. Boehme, G. Frenking, *Organometallics* **2000**, *19*, 571.
- [40] Y. Chen, G. Frenking, *J. Chem. Soc., Dalton Trans.* **2001**, 434.
- [41] T. Bollwein, P. J. Brothers, H. L. Hermann, P. Schwertfeger, *Organometallics* **2002**, *21*, 5236.
- [42] J. Uddin, G. Frenking, *J. Am. Chem. Soc.* **2001**, *123*, 1683.
- [43] C. Boehme, J. Uddin, G. Frenking, *Coord. Chem. Rev.* **2000**, *197*, 249.
- [44] G. Frenking, N. Fröhlich, *Chem. Rev.* **2000**, *100*, 717.
- [45] S. Aldridge, A. Rossin, D. L. Coombs, D. J. Willock, *Dalton Trans.* **2004**, 2649.
- [46] K. K. Pandey, A. Lledós, F. Maseras, *Organometallics* **2009**, *28*, 6442.
- [47] K. K. Pandey, D. G. Musaev, *Organometallics* **2010**, *29*, 142.
- [48] A. D. Becke, *Phys. Rev. A* **1988**, *38*, 3098.
- [49] J. P. Perdew, *Phys. Rev. B* **1986**, *33*, 8822.
- [50] a) C. Chang, M. Pelissier, Ph. Durand, *Phys. Scr.* **1986**, *34*, 394; b) J.-L. Heully, I. Lindgren, E. Lindroth, S. Lundquist, A.-M. Martensson-Pendrill, *J. Phys. B* **1986**, *19*, 2799; c) E. van Lenthe, E. J. Baerends, J. G. Snijders, *J. Chem. Phys.* **1993**, *99*, 4597; d) E. van Lenthe, E. J. Baerends, J. G. Snijders, *J. Chem. Phys.* **1996**, *105*, 6505; e) E. van Lenthe, R. van Leeuwen, E. J. Baerends, J. G. Snijders, *Int. J. Quantum Chem.* **1996**, *57*, 281; f) E. van Lenthe, A. E. Ehlers, E. J. Baerends, *J. Chem. Phys.* **1999**, *110*, 8943.
- [51] J. G. Snijders, E. J. Baerends, P. Vernooijs, *At. Data Nucl. Data Tables* **1982**, *26*, 483.
- [52] E. J. Baerends, D. E. Ellis, P. Ros, *Chem. Phys.* **1973**, *2*, 41.
- [53] J. Krijn, E. J. Baerends, *Fit Functions in the HFS-Method*, Internal Report (in Dutch), Vrije Universiteit Amsterdam, The Netherlands, **1984**.
- [54] E. J. Baerends, J. A. Autschbach, A. Berces, C. Bo, P. M. Boerigter, L. Cavallo, D. P. Chong, L. Deng, R. M. Dickson, D. E. Ellis, L. Fan, T. H. Fischer, C. Fonseca Guerra, S. J. A. van Gisbergen, J. A. Groeneveld, O. V. Gritsenko, M. Grüning, F. E. Harris, van den P. Hoek, H. Jacobsen, G. van Kessel, F. Kootstra, E. van Lenthe, V. P. Osinga, S. Patchkovskii, P. H. T. Philipsen, D. Post, C. C. Pye, W. Ravenek, P. Ros, P. R. T. Schipper, G. Schreckenbach, J. G. Snijders, M. Sola, M. Swart, D. Swerhone, G. te Velde, P. Vernooijs, L. Versluis, O. Visser, E. Wezenbeek, G. Wiesenekker, S. K. Wolff, T. K. Woo, T. Ziegler, *ADF*, 2008-01, Scientific Computing & Modelling NV, The Netherlands, **2008**.
- [55] a) K. Morokuma, *J. Chem. Phys.* **1971**, *55*, 1236; b) K. Morokuma, *Acc. Chem. Res.* **1977**, *10*, 294.
- [56] a) T. Ziegler, A. Rauk, *Theor. Chim. Acta* **1977**, *46*, 1; b) T. Ziegler, A. Rauk, *Inorg. Chem.* **1979**, *18*, 1558; c) T. Ziegler, A. Rauk, *Inorg. Chem.* **1979**, *18*, 1755.
- [57] F. M. Bickelhaupt, N. J. R. van Eikema Hommes, C. F. Guerra, E. J. Baerends, *Organometallics* **1996**, *15*, 2923.
- [58] A. Diefenbach, M. B. Bickelhaupt, G. Frenking, *J. Am. Chem. Soc.* **2000**, *122*, 6449.
- [59] K. K. Pandey, *Coord. Chem. Rev.* **2009**, *253*, 37.

- [60] K. K. Pandey, A. Lledós, *Inorg. Chem.* **2009**, *48*, 2748.
- [61] A. E. Reed, L. A. Curtiss, F. Weinhold, *Chem. Rev.* **1988**, *88*, 899.
- [62] G. Schaftenaar, *MOLDEN 3.4 CAOSCamm Center*, The Netherlands, **1998**.
- [63] a) A. F. Wells, *Structural Inorganic Chemistry*, 5th ed., Clarendon, Oxford, **1984**; b) L. Pauling, *The Nature of the Chemical Bond*, 3rd ed., Cornell University Press, Ithaca, NY, **1960**.
- [64] L. Pauling, *The Nature of the Chemical Bond*, 3rd ed., Cornell University Press, New York, **1960**, p. 239: the relationship of bond order to length is given by $d_n = d_1 - 0.71 \log(n)$ where n is the bond order, d_1 and d_n are the lengths of bonds with bond order 1 and n , respectively.
- [65] K. A. Wiberg, *Tetrahedron* **1968**, *24*, 1083.

Received: November 15, 2010

Published Online: March 24, 2011